Toward Fractioning of Isomers through Binding-Induced Acceleration of Azobenzene Switching

Rosaria Vulcano,[†] Paolo Pengo,[‡] Simone Velari,[§] Johan Wouters,[†] Alessandro De Vita,[∥,§] Paolo Tecilla,[‡] and Davide Bonifazi*[,⊥,†]

[†]Department of Chemistry, University of Namur (UNamur), Rue de Bruxelles 61, Namur, 5000, Belgium

[‡]Department of Chemical and Pharmaceutical Sciences and [§]Department of Engineering and Architecture, University of Trieste, Piazzale Europa 1, Trieste 34127, Italy

[∥]Department of Physics, King's College London, Strand, London WC2R 2LS, United Kingdom

[⊥]School of Chemistry, Cardiff University, Main Building, Park Place, Cardiff CF10 3AT, United Kingdom

Ⓢ Supporting Information

ABSTRACT: The E/Z isomerization process of a uracil–azobenzene derivative in which the nucleobase is conjugated to a phenyldiazene tail is studied in view of its ability to form triply H-bonded complexes with a suitably complementary 2,6-diacetyla-mino-4-pyridine ligand. UV–vis and ^1H NMR investigations of the photochemical and thermal isomerization kinetics show that the thermal $Z \rightarrow E$ interconversion is 4-fold accelerated upon formation of the H-bonded complex. DFT calculations show that the formation of triple H-bonds triggers a significant elongation of the N═N double bond, caused by an increase of its $\pi_g{}^*$ antibonding character. This results in a reduction of the N═N torsional barrier and thus in accelerated thermal $Z \rightarrow E$ isomerization. Combined with light-controlled $E \rightarrow Z$ isomerization, this enables controllable fractional tuning of the two configurational isomers.

binding-induced acceleration and fractioning
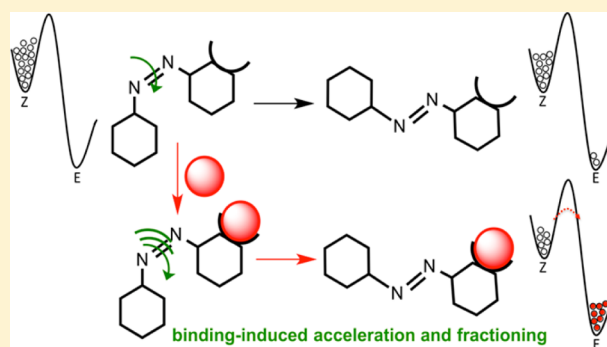
INTRODUCTION

Isomerization is the process by which one molecule is transformed into another molecule that has exactly the same atoms, but with a different arrangement.[1,2] In artificial systems, it is usually an external stimulus (e.g., light, electrochemical or thermal inputs, cf. path A, Scheme 1) that triggers such configuration interconversion.[3−6] A typical example is the E/Z photoisomerization of the azobenzene scaffold, for which the single isomer can be selectively produced by the relevant light excitation[3,7−9] or electrochemical[10] input. This is certainly one of the most studied functional groups allowing spatiotemporal control of the conformational and overall structural properties of molecular systems.[11−13] Notable applications include the fabrication of photoresponsive architectures in materials science[3,14−30] and biology.[31−35] Isomerization also plays a fundamental role in a number of naturally occurring biochemical processes.[36−38] For example, the cis−trans isomerization of amide bonds involving proline is an important step in the folding of proteins. Yet, being relatively slow, it is often rate-limiting.[39,40] To hasten it, Nature provides specific enzymes referred as "peptidyl-prolyl isomerases" that through binding of the relevant amino acids trigger the switching at the N-terminal amide bond of proline (path B, Scheme 1).[39]

Systems that respond to both stimuli- and binding-induced mechanisms of isomerization or switching are, however, more

Scheme 1. General Scheme for a Dual Stimuli- and Binding-Triggered Isomerization System[a]
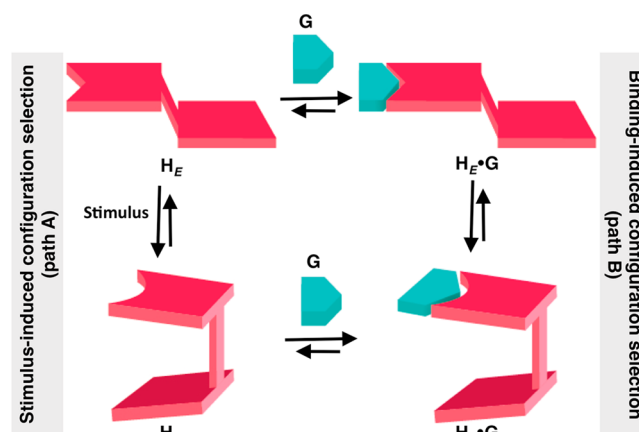
[a]H and G indicate the host and guest molecules, respectively, with the host adopting two different configurations (H_Z and H_E).

difficult to find (Scheme 1). Hecht and co-workers[41] developed a triple H-bonding motif whose association strength could be

1

modulated by the ring-closed switching state of a photochromic bis(thiazol-4-yl)maleimides. Switchable H-bonded host−guest complexes containing an azobenzene were developed by the groups of Goswami,[42] Rotello,[43] Gadhiri,[44] Hecht,[45] and Ballester.[46] The possibility of further modulating the isomerization process through noncovalent bonding was not explored in these previous works, and only examples describing the use of gold nanoparticles[47−49] have been described. This would be appealing, as it could give access to responsive architectures that in the presence of a binder might enable a controlled structural selection protocol capable of achieving a well-defined target complex structure in a desired concentration. This possibility is explored here, where our specific goal is to develop a complete dual stimuli- and binding-triggered isomerization cycle.

The Concept: Toward Fractionation of Isomers. Namely, we wish to investigate the possibility of controlling the relative molar fraction χ and $(1 - \chi)$ of the two configuration isomers of a molecule, with the goal of being able to tune these concentrations to arbitrary complementary values in the 0−1 range. We note that a range of χ values consistent with thermodynamic equilibrium could in principle be obtained by simply varying the temperature of the system and allowing the system to equilibrate, provided that the two isomers have different free energies. This, however, could be disruptive for the system if the temperatures required for the desired concentration were too high, while this approach would in all cases never achieve a higher concentration for the isomer of higher energy, which we wish to be able to do here. A second possibility would be to use complexation of the isomers to tune the energy levels of the two complexes, so to alter their equilibrium concentration without temperature adjustment. However, full tunability of χ in the 0−1 range would be lost in this case, unless an "almost continuum" range of complexes could be devised for this scope.

A different, simpler, and more interesting possibility is to achieve concentrations at "metastable" values outside thermodynamic equilibrium.[5] A necessary condition for this route to be allowed is that the two isomer states must correspond to local energy minima separated by energy barriers high enough to make any equilibrating transition negligibly slow. In this respect, the E/Z isomerization of azobenzene is certainly one of the most accessible reactions.[3] The (stable) E and the (metastable) Z isomers have separated energies, so that at equilibrium for all temperatures of interest the E isomer is the only present species. Furthermore, if some Z concentration is externally induced (e.g., by light), the thermal process bringing the system back to equilibrium occurs on a slow (hour) time scale, i.e., meets a "slow kinetics" requirement.[3] Under these circumstances, a shift of concentration out of the equilibrium value can be achieved by suitably photoactivating the $E \rightarrow Z$ (after which, $Z \rightarrow E$ is also viable), using an appropriate light frequency. Any Z concentration could, in principle, be achieved in this way by carefully dosing the photon flux and the irradiation time.

We can, however, conjecture that an alternative route to control the isomeric composition could be achieved by photo-inducing a complete $E \rightarrow Z$ transition and accelerating the $Z \rightarrow E$ back-transition process (Scheme 2, red arrow) only for a controllable fraction of the Z isomers. If the fast $Z \rightarrow E$ decaying isomers could be those that form a noncovalent complex with appropriately designed guest molecules, their fraction would be easily controlled by tuning the guest concentration. Once the fast, fractional Z to E back-conversion has occurred, all that is needed to "pin" the system indefinitely at the remaining (target) Z isomer fraction, is to correct for the slow drift toward

Scheme 2. Schematic Gibbs Free Energy Landscape Illustrating the General Principle of the E/Z Isomer Fractioning through Noncovalent Complexation
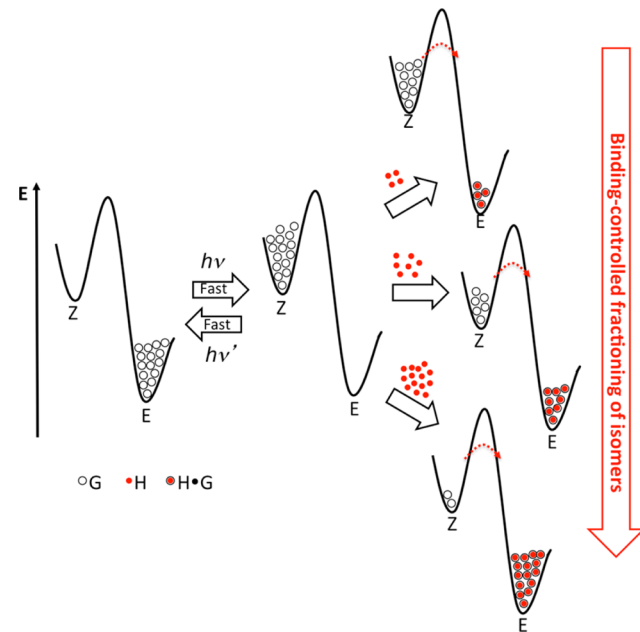
thermodynamic equilibrium. This can be easily achieved by further, time-sparse "refreshing" photoactivation steps.

Building on these hypotheses, here we report the first study of an azobenzene-like system whose isomerization properties are responsive to both a luminous stimulus and a noncovalent H-bonded recognition event. The idea is that a perturbation caused by the formation of a multiple H-bonded interaction should trigger a change of the photoisomerization behavior of the phenyldiazene moiety by modifying the energy barriers associated with isomers interconversion.

■ RESULTS AND DISCUSSION

Molecular Design and Solid-State Recognition Investigations. To engineer such a system, one needs to consider a structure in which the isomerizing unit is in direct conjugation with the recognition site. In this way, any changes occurring at one of the two moieties are then reflected on the other. Capitalizing on our previous achievements on the H-bonded uracil·2,6-diamidopyridine complex,[50−56] we therefore designed and synthesized a photoswitchable uracil−azobenzene derivative presenting direct anchoring of the phenyldiazenyl group to the nucleobase at either the 5- or 6-position (**5AUP** and **6AUP**, respectively, Figure 1).

This bridging was selected to favor the establishment of an effective electronic communication between the two moieties. As far as the synthesis is concerned, molecules **5AUP** and **6AUP** were prepared in a two-step pathway (see the SI). To improve the solubility of the molecular scaffold in organic solvents, we equipped the aryl and uracil rings with *tert*-butyl and N1-propyl substituents, respectively. *N*-Dialkylated analogue **5AUPP** (Figure 1) was also prepared as a reference molecule. To probe the H-bonding recognition properties of **5AUP** and **6AUP** we have used 2,6-diacetylamino-4-[(trimethylsilyl)ethynyl]pyridine (**DAP**) as complementary recognition unit (Figure 1).[50−52,56]

Suitable single crystals for X-ray diffraction analysis were grown by slow evaporation of a toluene solution containing a 1:1 mixture of the relevant uracil−azobenzene derivative and **DAP**.
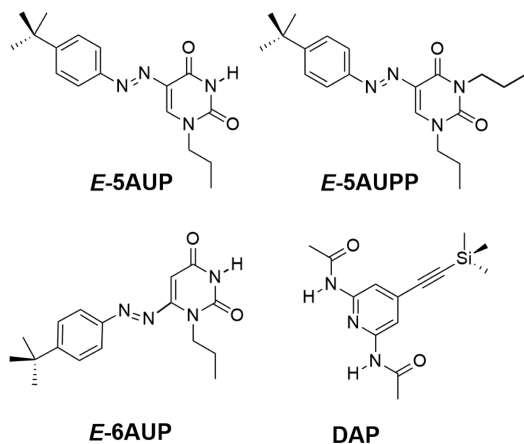
2

Figure 1. Molecular structures of the uracil−azobenzene derivatives.

As expected, the X-ray structure (Figure 2) reveals the presence of the H-bonded complex in which the E isomer of **5AUP** (**E-5AUP**) and **6AUP** (**E-6AUP**) engages triple H-bonding interactions with **DAP** (relevant distances for **E-5AUP·DAP**: 2.911, 3.064, and 2.931 Å for O1···N9, N3···N10, and O2···N11, respectively). These values are comparable to those previously reported for similar H-bonded complexes.[57,58] Any attempts to obtain the X-ray structure for the **Z-5AUP·DAP** and **Z-6AUP·DAP** complexes failed.

E/Z Isomerization Studies in Solution for the Uracil Derivatives. The electronic absorption spectrum of **5AUP** in toluene is depicted in Figure 3a. The molecule exhibits two UV absorption bands at 360 and 442 nm, which are attributed to $\pi-\pi^*$ (of the E isomer) and $n-\pi^*$ (of the Z isomer) electronic transitions, respectively.[59−61] When irradiated at 360 nm, remarkable changes are observed in the absorption spectra of **5AUP** (Figure 3b), with an intense and fast increase of a new band centered at around 300 nm and a substantial increase of the

intensity of the $n-\pi^*$ band at 442 nm with a concomitant disappearance of the $\pi-\pi^*$ absorption. Neat isosbestic points are maintained throughout the photoirradiation experiments, showing the clean occurrence of the nearly quantitative $E \rightarrow Z$ isomerization. Thermal $Z \rightarrow E$ interconversion producing the most thermodynamically stable E isomer occurs very slowly as shown in Figure 3c (see also below). On the other hand, irradiation at 442 nm causes a fast $Z \rightarrow E$ isomerization, resulting in a decrease of the $n-\pi^*$ absorption and a full restoration of the $\pi-\pi^*$ band (Figure 4a). Repetitive photoinduced switching cycles evidenced an excellent fatigue resistance and remarkable photostability of the system (Figure 4b). Taken together, these data suggest that the substitution of the phenyl ring with the nucleobase has little influence on the photochemical properties, with **5AUP** showing the typical E/Z switching behavior of the archetypal azobenzene.[61,62]

When looking at the photoisomerization of **6AUP**, the characteristic azobenzene bands are no longer distinguishable in the absorption spectrum of this regioisomer (Figure 3e). Likely in **6AUP**, the azobenzene unit is involved in a 1,4-type conjugation with the carbonyl group of the uracil moiety. When irradiated at 360 nm, the absorption band in the 300−400 nm spectral region decreases, reaching saturation after 3 min of irradiation. The weak features of the Z isomer seem to be sub-stantially masked within the strong absorption envelope of the conjugated molecule. When left into the dark, full recovery of the initial absorption spectra is obtained after 20 min. Together with the possibility of reaching nearly quantitate two-way isomer-ization, these data suggest that the slower reaction dynamics of **5AUP** make this regioisomer the best candidate to intercept both configurational isomers and study their binding properties with **DAP** in solution with classical spectroscopic techniques like ^{1}H NMR. For this reason, only regioisomer **5AUP** has been used to perform the binding studies.

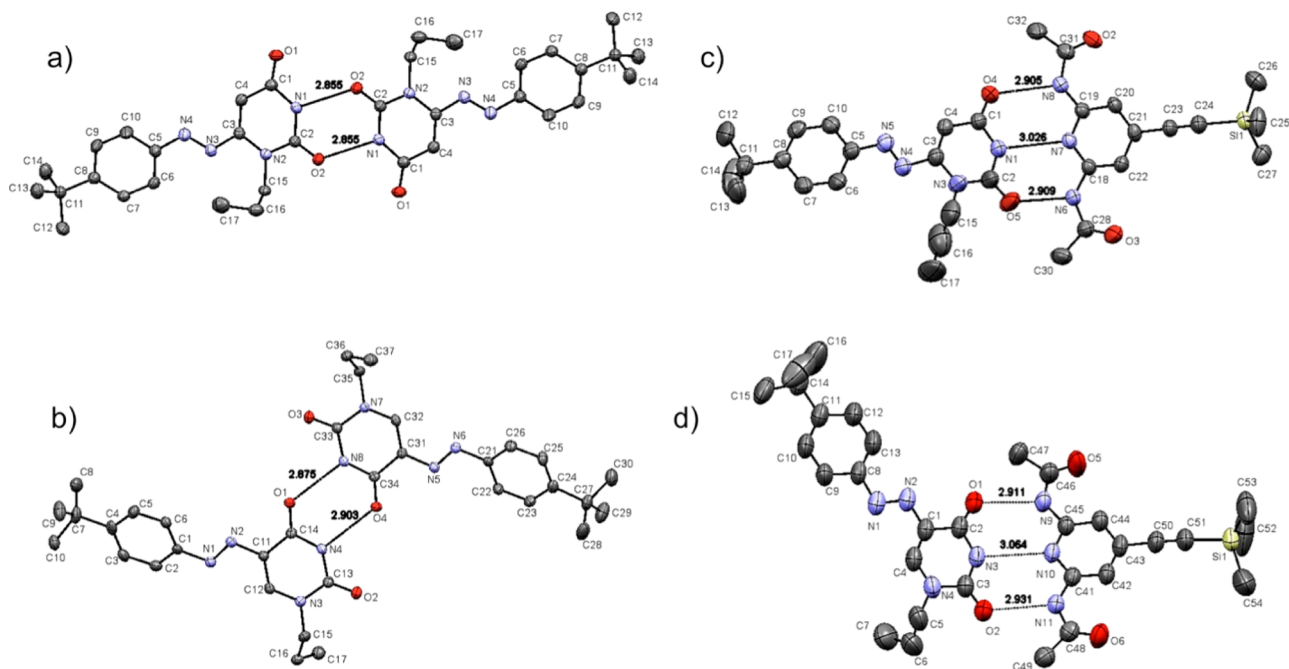**E/Z Isomerization and Binding Studies for the Supra-molecular Complexes in Solution.** To shed further light on

Figure 2. ORTEP representation of the X-ray structures of (a) **E-6AUP**, (b) **E-5AUP**, (c) **E-6AUP·DAP** and (d) **E-5AUP·DAP**. The space groups are P-1, P2$_1$/n, P-1, and P2$_1$/c for a, b, c, and d, respectively.

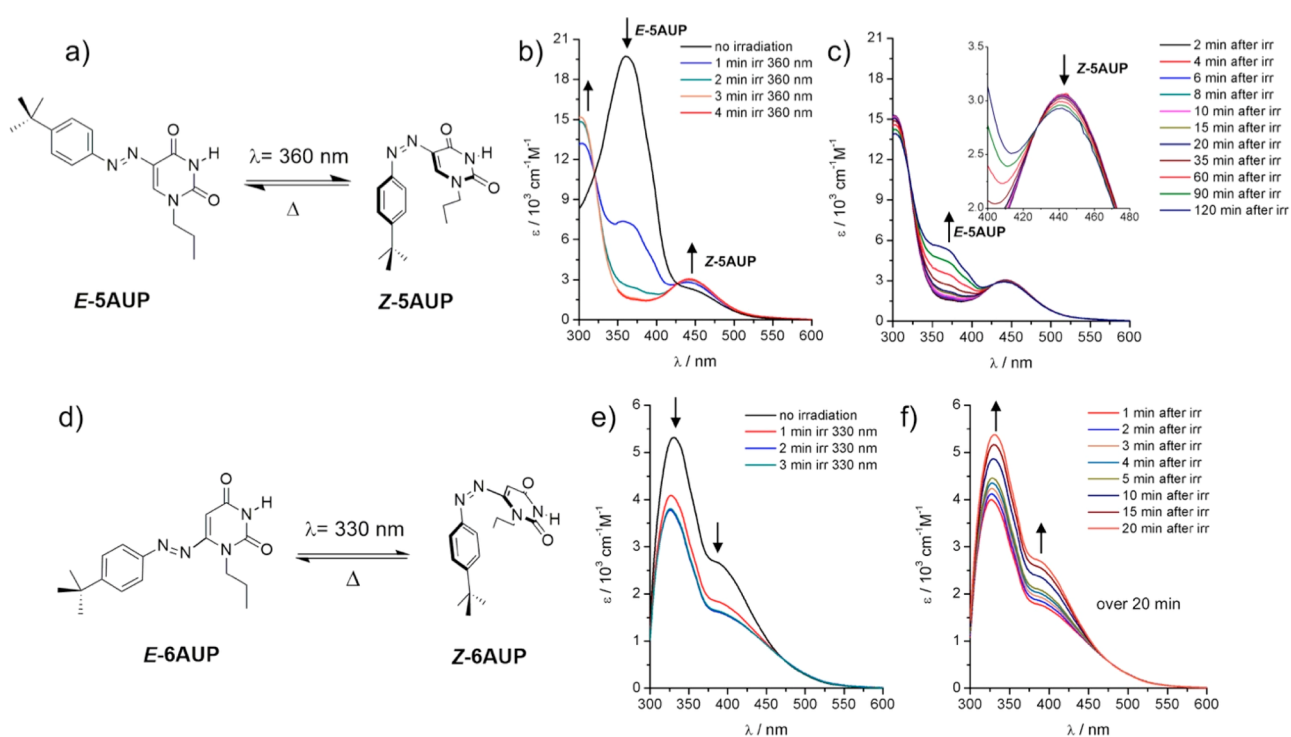**Figure 3.** E/Z isomerization equilibria for **5AUP** (a) and **6AUP** (d) in toluene. Photo E → Z (b and e) and thermal Z → E (c and f) isomerization of **5AUP** (2.5 × 10⁻⁵ M) and **6AUP** (5.4 × 10⁻⁵ M) in toluene at 25 °C. Inset: zoom in the n−π* absorption region. The thermal Z → E isomerization was followed over 120 and 20 min periods for **5AUP** and **6AUP**, respectively.
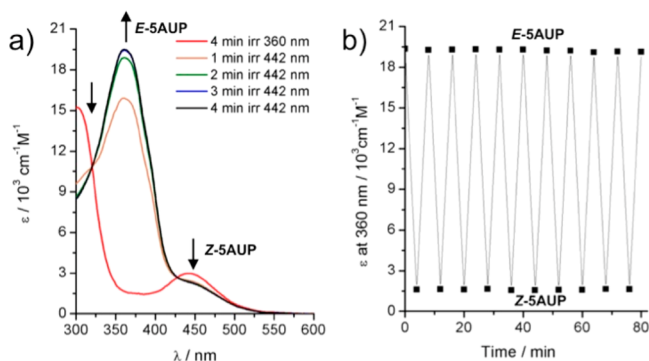

Figure 4. (a) Z → E photoisomerization of **5AUP** (2.5 × 10⁻⁵ M); (b) repetitive photoinduced switching cycles of **5AUP** obtained by alternating irradiation at 360 and 442 nm.

the recognition properties of **5AUP** in solution, ¹H NMR titration and Job's plot analysis were performed for both Z and E isomers to estimate the association constants (K_i) and the binding stoichiometry in solution. In both cases, increasing the concentration of **DAP** caused a progressive downfield shift of the uracil NH proton under a regime of fast equilibrium exchange (Figure 5). As evidenced at the solid state, the Job's plots analysis confirmed the 1:1 binding stoichiometry in solution for the **5AUP·DAP** complex (see the SI). The association constant (K_E, calculated through the data fitting with Dynafit software[63]) for the **E-5AUP·DAP** complex was found to be 6710 ± 800 M⁻¹, which is half of that measured for the reference **Upr·DAP** complex under the same experimental conditions (see the SI). This is in line with the literature findings obtained for other uracil-derived molecular scaffolds in toluene.[50]

Regarding the **Z-5AUP·DAP** complex, the titration experiments (Figure 6) were performed in the dark at constant

temperature (T = 298 K) with a freshly, light-isomerized solution of **5AUP** (δ_{NH} = 7.5 ppm for the imide proton in the absence of **DAP**, and no presence of **E-5AUP** was detected at the beginning of the titration). By adding increasing amounts of **DAP**, two different NH proton resonances began to appear, reaching the saturation chemical shift values of 12.1 and 11.7 ppm after the addition of 3.4 equiv of **DAP** (Figure 6). Considering the chemical shifts observed during the titration experiments performed for **E-5AUP·DAP**, the resonances at lower fields are attributed to **E-5AUP**, while those at higher fields are attributed to the Z isomer. Upon increasing additions of **DAP**, the intensity of the imide proton signal for the E isomer increases at the expenses of that pertaining to the Z isomer, which suggests Z → E interconversion (Figure 6). As one can notice, this gives rise to defined fractions of the two isomers depending on the **DAP** concentration. For instance at [**DAP**]/[**5AUP**] ratios of 0.2, 0.5, and 2 the molar fractions (χ_E) of the E isomer (free and complexed) are 0.21, 0.34, and 0.66, respectively (Figure 6). Because of this thermal Z → E interconversion, the estimation of the association constant (K_Z) for the **Z-5AUP·DAP** complex was revealed to be less straightforward as its concentration is interconnected with the progressive increase of the other complex, namely **E-5AUP·DAP**. The fitting model (applied with Dynafit software) employed for estimating the association constant need to use as independent variables the concentration of **DAP** and that of the two isomers (measured from the integration of the imidic proton resonances). Using the K_E value estimated from the titration experiments of **E-5AUP**, we could estimate the K_Z value for the **Z-5AUP·DAP** complex to be 4040 ± 355 M⁻¹. Notably, this is almost half of that measured for its isomer **E-5AUP·DAP**.

The rate constant of thermal Z → E isomerization for **5AUP** was investigated in the dark by both UV−vis and ¹H NMR measurements. The UV−vis experiment shows an increasing of
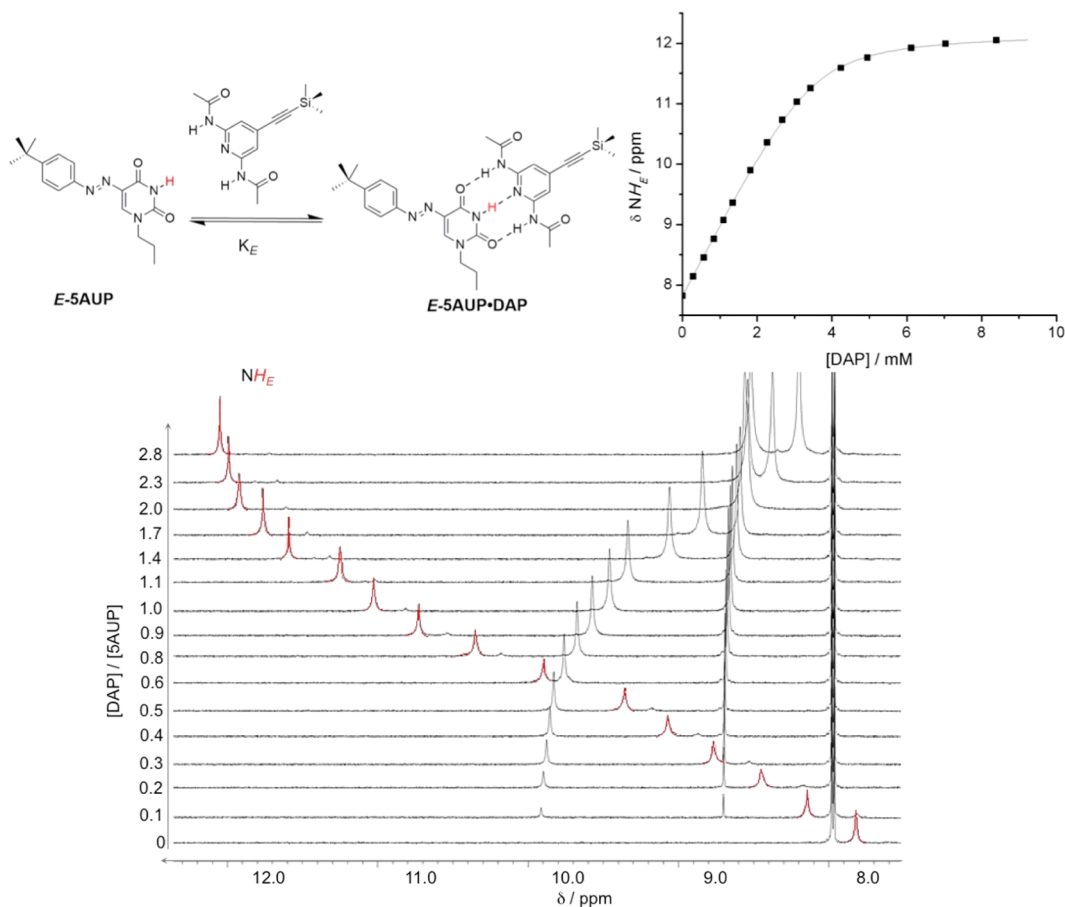
4

Figure 5. Dark ^{1}H NMR titrations of *E*-5AUP (3.0 mM in toluene-d_8) upon addition of increasing amounts of **DAP** at 25 °C. The red signal corresponds to the imide proton of the uracil unit in free *E*-5AUP (δ_{NH} = 7.8 ppm) and in *E*-5AUP·DAP complex (δ_{NH} = 12.1 ppm after addition of 2.8 equiv of **DAP**), respectively.

the absorbance at 360 nm over time, corresponding to the increasing of the concentration for the *E* isomer (Figure 7a). The process follows a first order kinetic equation with a rate constant (k_{est}) value of $(2.7 \pm 0.01) \times 10^{-5}$ s^{-1} ($t_{1/2}$ = 7.1 h, see the SI). The ^{1}H NMR analysis was restricted to the first instants of the reaction according to the initial rate method (Figure 7b). The k_{est} value obtained from ^{1}H NMR measurements corresponds to $(2.5 \pm 0.2) \times 10^{-5}$ s^{-1}, which is in good agreement with the value obtained from the UV−vis measurements. As a control experiment, we have studied the thermal $Z \rightarrow E$ isomerization of the reference dialkylated uracil derivative (5AUPP), where also the $N(3)$ position bears a propyl chain. The k_{est} value obtained from UV−vis measurements corresponds to $(3.06 \pm 0.03) \times 10^{-5}$ s^{-1} (see the SI), which is consistent with that calculated for the $Z \rightarrow E$ conversion of 5AUP in the absence of **DAP**.

To understand if the supramolecular interaction has an influence on the thermal $Z \rightarrow E$ isomerization rate, further ^{1}H NMR investigations have been made using *Z*-5AUP solutions in the presence of variable **DAP** concentrations (Figure 8). In the presence of a large excess of **DAP**, the maximum concentration of complex (about 96%) is achieved (Figure 8b). This allows calculation of the rate constant of the thermal $Z \rightarrow E$ isomerization process within the complex 5AUP·DAP, which was found to be $(1.0 \pm 0.3) \times 10^{-4}$ s^{-1} (see the SI). It is now apparent that the $Z \rightarrow E$ isomerization process within the complex is about four times faster than that occurring for 5AUP alone $(2.5 \pm 0.2 \times 10^{-5}$ s$^{-1})$.

Scheme 3 summarizes the relevant equilibria and kinetic processes involving the *Z*-5AUP and *E*-5AUP isomers along with their complexes with **DAP**. The isomer fractioning concept implies the photogeneration of *Z*-5AUP in the presence of a given concentration of **DAP**. The fast isomerization within the H-bonded complex will produce a *Z*/*E* mixture with an isomeric composition determined by the amount of *Z*-5AUP·DAP complex and subjected to a drift toward the thermodynamic equilibrium composition due to the slower background thermal isomerization of free *Z*-5AUP. As a consequence, the possibility of producing a *Z*/*E* mixture with a defined isomeric composition and stable in time depends on the k_{iso}/k_{est} ratio. On the other hand, since the equilibration of **DAP** between the two 5AUP isomers is fast on the isomerization time scale, this process should not influence the system which experiences a time-averaged composition ruled by the association constants. In our case, the k_{iso}/k_{est} ratio is about 4. Although this acceleration does not to allow a complete separation between the two kinetic processes, a simulation shows that, for example, starting from a 1:1 mixture of *Z*-5AUP/DAP after about 10 h the complex is fully isomerized but the χ_E (free and complexed) is 0.78 with the amount exceeding the 50% derived from the interconversion of the free *Z*-5AUP. However, the isomeric composition obtained is relatively stable in time. For instance, after 5 h the χ_E value changed by only 0.09, going from 0.78 to 0.87.

Theoretical Rationale. To shed further light on the causes affecting the acceleration of the switching process, we have performed density functional theory (DFT) calculations using
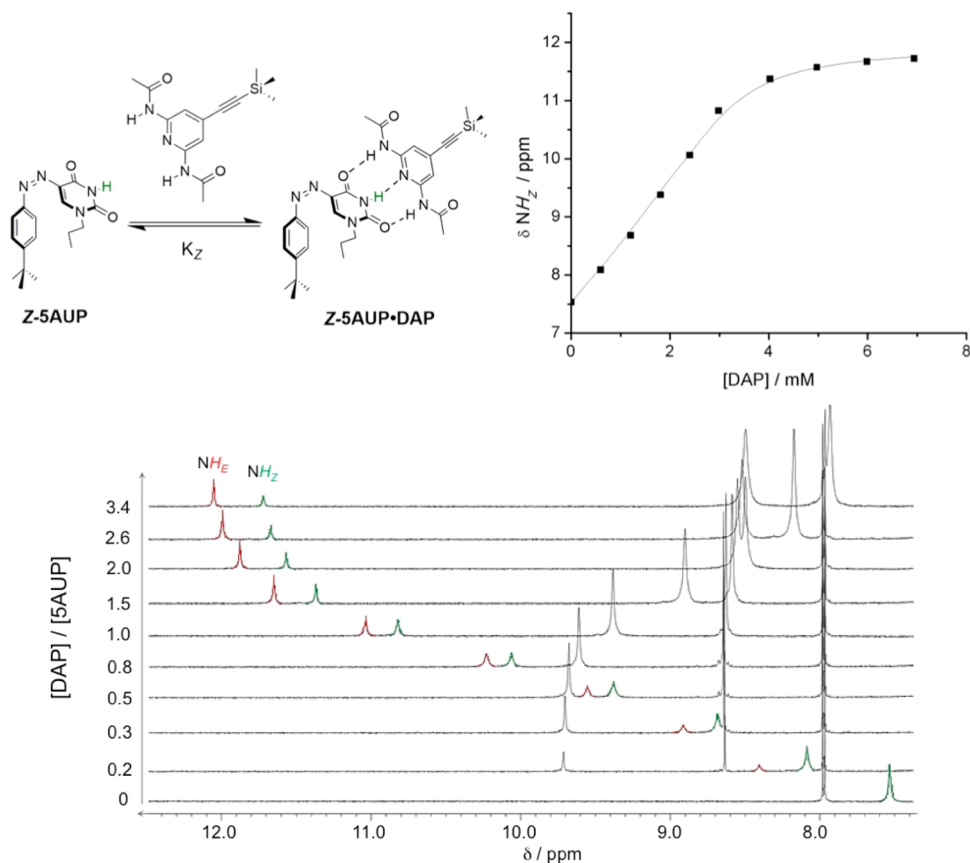
5

Figure 6. Dark ^{1}H NMR titrations of **Z-5AUP** obtained after irradiation at 360 nm of the **5AUP** sample (3.8 mM in toluene-d_8) upon addition of increasing amounts of **DAP** at 25 °C. The green and red signals correspond to the imide proton of the uracil core in the **Z-5AUP** and **E-5AUP** containing species, respectively.
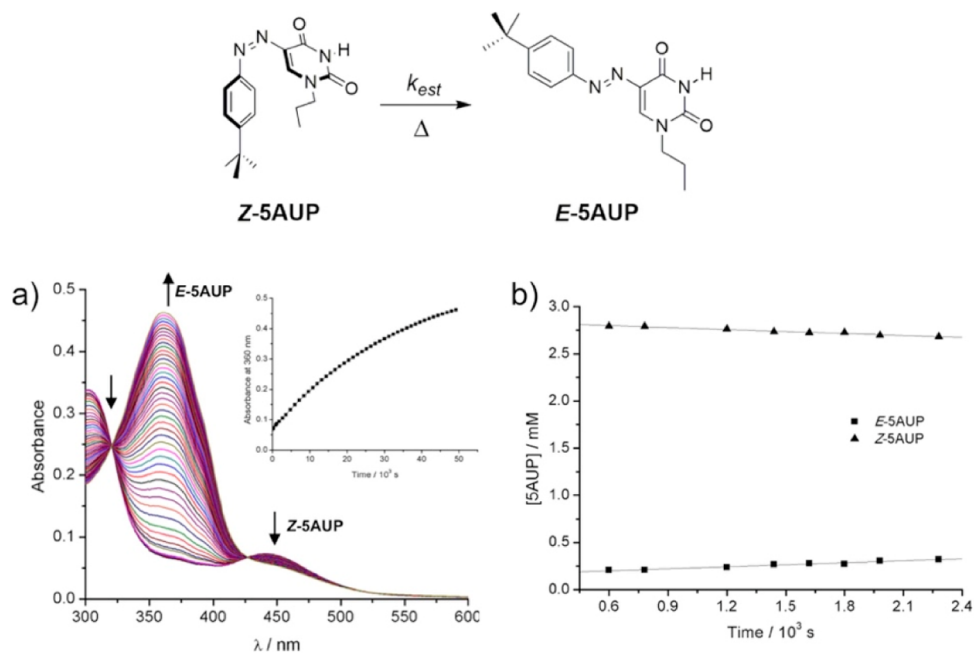

Figure 7. (a) UV−vis measurements of the thermal $Z \rightarrow E$-**5AUP** isomerization at 25 °C after sample irradiation at 360 nm (3.0×10^{-5} M toluene solution); (b) time-dependent variation of the concentration of the isomers estimated from the integrals of the NCH$_2$ protons peaks area as measured by ^{1}H NMR after sample irradiation at 360 nm (3.0×10^{-3} M toluene-d_8 solution).

the PWSCF code of the Quantum ESPRESSO distribution[64] and the Perdew−Burke−Ernzehof (PBE) functional,[65] which was used previously in careful studies of similar systems.[66,67] First, we optimized the gas-phase structures of **DAP**, **Z-5AUP**, and **E-5AUP** molecules and those of their **Z**- and **E-5AUP·DAP** complexes (see the SI). The calculations confirm the higher
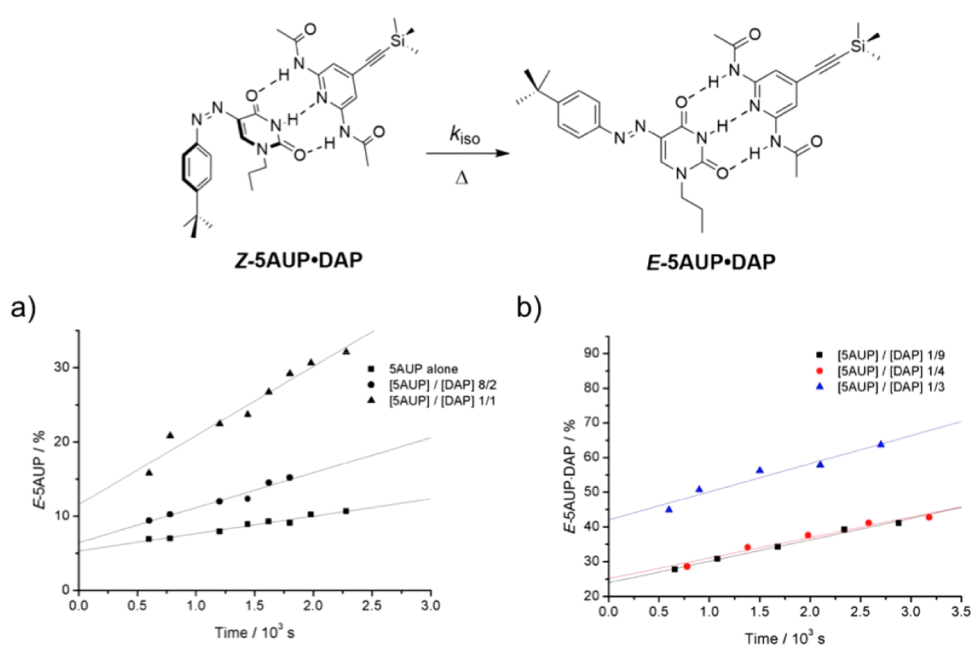
Figure 8. (a) Kinetic profiles of the thermal $Z \rightarrow E$ isomerization of **5AUP** in toluene-d_8 in the absence and in the presence of different **DAP** concentrations measured by ^{1}H NMR at 25 °C after sample irradiation at 360 nm; (b) kinetic profiles of the thermal $Z \rightarrow E$ isomerization of **5AUP·DAP** complex in the presence of exceeding quantities of **DAP** measured by ^{1}H NMR at 25 °C in toluene-d_8 after sample irradiation at 360 nm. Initial sample concentrations: (■) $[\text{5AUP}]_0 = 1.0 \times 10^{-3}$ M, $[\text{DAP}]_0 = 9.4 \times 10^{-3}$ M ; (●) $[\text{5AUP}]_0 = 2.2 \times 10^{-3}$ M, $[\text{DAP}]_0 = 9.6 \times 10^{-3}$ M, and (▲) $[\text{5AUP}]_0 = 3.2 \times 10^{-3}$ M, $[\text{DAP}]_0 = 10.2 \times 10^{-3}$ M.

Scheme 3. Summary of the Relevant Complexation Equilibria and Isomerization Kinetics Involving 5AUP and DAP
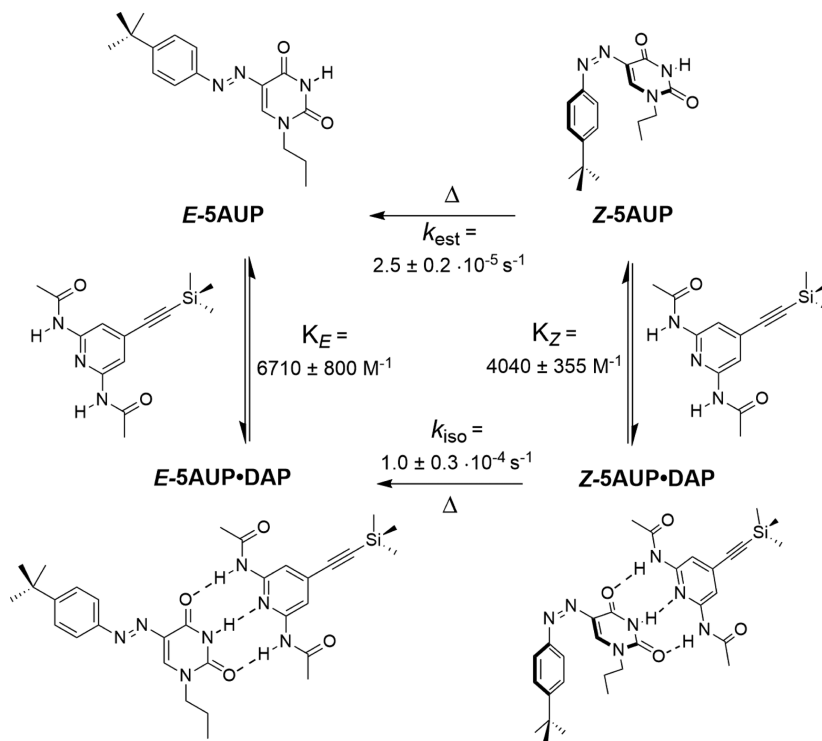
stability of the E isomers with respect to that of the Z both in free and complex species. In particular, the calculated energy of the metastable Z isomer is 0.65 and 0.61 eV higher than the E level for **5AUP** and **5AUP·DAP**, respectively. As expected, these energy differences between this configurational isomers are comparable with the values previously computed for azobenzene by DFT techniques (0.66 eV) as well as a broad range of

techniques including highly sophisticated coupled-cluster and diffusion Monte Carlo techniques (0.52−0.73 eV).[67] Analysis of our DFT results suggests a peculiar redistribution of the electron density, which occurs around the N≡N bond upon forma-tion of the complex of **Z-5UAP** molecule. This is visible in Figure 9, where the electron density difference $\rho_{tot} - \Sigma\rho_{mol}$ is shown, portraying the electron density readjustment following
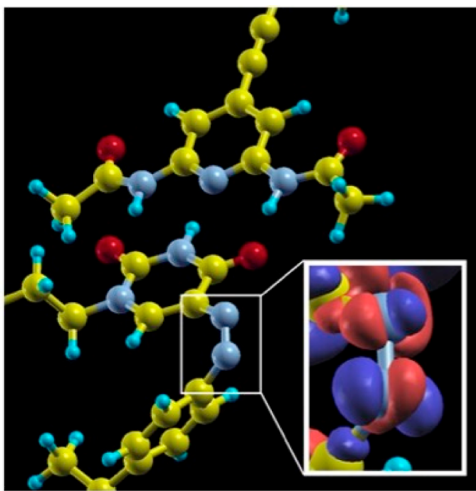
7

Figure 9. Side view of the optimized structure of **Z-5AUP·DAP**. The zoomed region displays the change of the calculated electron density in the N=N bond region of **Z-5AUP** upon complexation with **DAP** (electron density accumulation is depicted in red and depletion in blue).

process and a nearly quantitate two-way isomerization. In the presence of a 2,6-diamidopyridine, triply H-bonded complexes were formed both in solution and at the solid state. UV−vis and ^{1}H NMR investigations of the photochemical and thermal isomerization kinetics in toluene solutions showed that the thermal $Z \rightarrow E$ interconversion is 4-fold accelerated upon formation of the H-bonded complex when compared to that of the uracil derivative alone. DFT calculations suggest that the formation of the triply H-bonded complex trigger weakening and elongation of the N=N double bond through increase of its π_g^* antibonding character. This is expected to reduce the N=N torsional barrier and thus rationalize the acceleration of the thermal $Z \rightarrow E$ isomerization. This binding-induced acceleration of the isomerization process was found to give access to tailored isomers fractions (χ) with limited variation of the mixture over a few hours, although in our system the acceleration factor is rather small to ensure a complete time separation of the two kinetic processes. Structural modifications of the aza derivative are currently under investigation to increase the gap between the isomerization rates within and outside the complex. Such types of systems are indeed of great appeal as they could give access to responsive architectures, which upon exposition to an external stimulus undergo a structural perturbation (e.g., unfolding, unzipping, and denaturation).[72−75] This reactive state could eventually develop into a new minimum in the presence of the relevant binder (e.g., drugs, nucleic acid strand, enzyme active sites, and metabolites), the concentration of which can control both structure and its fraction. For instance, this modified system could be used to design photoresponsive nucleic acids that could undergo controlled unfolding and folding of DNA helixes,[76] possibly opening new horizons into light-triggered gene manipulation.

the "switching on" of the interaction between the two molecules in the complex (ρ_{tot} is the electron density of the complex and $\Sigma\rho_{mol}$ is the sum of the densities of the two isolated single molecules with same atomic position, in the gas phase). The alternated lobes of opposite signs (Figure 9, inset) fingerprints the onset of hybridization of electronic states, mixing states with π_g^* antibonding orbital components with bonding molecular states that do not have a nodal plane between the two N atoms of the C−N=N−C moiety. This is expected to lower the torsional barrier associated with the C−N=N−C group upon formation of the **Z-5UAP·DAP** complex, consistent with the experimental observations.

Finally, in an effort to estimate the effect of complexation on the $Z \rightarrow E$ isomerization barrier, we investigated the **Z-5AUP·DAP** $\rightarrow$ **E-5AUP·DAP** and the **Z-5AUP** $\rightarrow$ **E-5AUP** conversions, using the nudged elastic band technique[68−70] to model the transition barrier. We note that solvent effects as well as temperature effects should be fully included to properly account for the enthalpic and entropic contributions that define the free energy barrier relevant to the experimental interconversion conditions. While some techniques exist that could capture complex electron−phonon dynamics and level crossing occurring in system like the present ones during the isomerization transition,[71] a simple estimate of the barrier lowering upon DAP complexation relying on error cancellation can be obtained from our DFT static potential energy results. These suggest that the Z to E barrier gets smaller upon **Z-5AUP** complexation with **DAP**. Our computed 60 meV energy barrier reduction value (which would correspond to a speed-up factor of about 10 at 300 K) is furthermore comparable with the 34 meV free energy barrier reduction value (corresponding to the experimentally observed speedup of about 4) obtained from the ratio of our experimental thermal conversion rates further assuming the same attempt rate for the $Z \rightarrow E$ conversion in free **Z-5AUP** and H-bonded complex **Z-5AUP·DAP**.

CONCLUSIONS

In conclusion, in this work we have synthesized photoswitchable uracil−azobenzene conjugates presenting direct anchoring of the phenyldiazenyl group to the uracil nucleobase, with the 5-functionalized derivatives depicting a slow thermal switching

ASSOCIATED CONTENT

● **Supporting Information**

X-ray data for compound 5AUP (ZIP)
X-ray data for compound 5AUP·DAP (ZIP)
X-ray data for compound 6AUP (ZIP)
X-ray data for compound 6AUP·DAP (ZIP)
Synthetic protocols and spectroscopic characterizations (PDF)

AUTHOR INFORMATION

Corresponding Author
*bonifazid@cardiff.ac.uk
ORCID
Davide Bonifazi: 0000-0001-5717-0121
Notes
The authors declare no competing financial interest.

ACKNOWLEDGMENTS

■ REFERENCES

(1) Dugave, C.; Demange, L. *Chem. Rev.* **2003**, *103*, 2475.
(2) Hassam, M.; Taher, A.; Arnott, G. E.; Green, I. R.; van Otterlo, W. A. L. *Chem. Rev.* **2015**, *115*, 5462.
(3) Bléger, D.; Hecht, S. *Angew. Chem., Int. Ed.* **2015**, *54*, 11338.
(4) Mukhopadhyay, R. D.; Praveen, V. K.; Ajayaghosh, A. *Mater. Horiz.* **2014**, *1*, 572.
(5) Kathan, M.; Hecht, S. *Chem. Soc. Rev.* **2017**, *46*, 5536.
(6) Klajn, R. *Chem. Soc. Rev.* **2014**, *43*, 148.
(7) Hartley, G. S. *Nature* **1937**, *140*, 281.
(8) Moreno, J.; Gerecke, M.; Grubert, L.; Kovalenko, S. A.; Hecht, S. *Angew. Chem., Int. Ed.* **2016**, *55*, 1544.
(9) Yagai, S.; Karatsu, T.; Kitamura, A. *Chem. - Eur. J.* **2005**, *11*, 4054.
(10) Goulet-Hanssens, A.; Utecht, M.; Mutruc, D.; Titov, E.; Schwarz, J.; Grubert, L.; Bléger, D.; Saalfrank, P.; Hecht, S. *J. Am. Chem. Soc.* **2017**, *139*, 335.
(11) Bléger, D.; Schwarz, J.; Brouwer, A. M.; Hecht, S. *J. Am. Chem. Soc.* **2012**, *134*, 20597.
(12) Klajn, R. *Pure Appl. Chem.* **2010**, *82*, 2247.
(13) Zeitouny, J.; Aurisicchio, C.; Bonifazi, D.; De Zorzi, R.; Geremia, S.; Bonini, M.; Palma, C.-A.; Samorì, P.; Listorti, A.; Belbakra, A.; Armaroli, N. *J. Mater. Chem.* **2009**, *19*, 4715.
(14) Liaros, N.; Couris, S.; Maggini, L.; De Leo, F.; Cattaruzza, F.; Aurisicchio, C.; Bonifazi, D. *ChemPhysChem* **2013**, *14*, 2961.
(15) Maggini, L.; Marangoni, T.; Georges, B.; Malicka, J. M.; Yoosaf, K.; Minoia, A.; Lazzaroni, R.; Armaroli, N.; Bonifazi, D. *Nanoscale* **2013**, *5*, 634.
(16) Weber, C.; Liebig, T.; Gensler, M.; Zykov, A.; Pithan, L.; Rabe, J. P.; Hecht, S.; Bléger, D.; Kowarik, S. *Sci. Rep.* **2016**, *6*, 25605.
(17) Bléger, D.; Ciesielski, A.; Samorì, P.; Hecht, S. *Chem. - Eur. J.* **2010**, *16*, 14256.
(18) Lee, J.; Klajn, R. *Chem. Commun.* **2015**, *51*, 2036.
(19) Kundu, P. K.; Klajn, R. *ACS Nano* **2014**, *8*, 11913.
(20) Klajn, R.; Browne, K. P.; Soh, S.; Grzybowski, B. A. *Small* **2010**, *6*, 1385.
(21) Mahesh, S.; Gopal, A.; Thirumalai, R.; Ajayaghosh, A. *J. Am. Chem. Soc.* **2012**, *134*, 7227.
(22) Gopal, A.; Hifsudheen, M.; Furumi, S.; Takeuchi, M.; Ajayaghosh, A. *Angew. Chem., Int. Ed.* **2012**, *51*, 10505.
(23) Rajaganesh, R.; Gopal, A.; Mohan Das, T.; Ajayaghosh, A. *Org. Lett.* **2012**, *14*, 748.
(24) Das, S.; Ranjan, P.; Maiti, P. S.; Singh, G.; Leitus, G.; Klajn, R. *Adv. Mater.* **2013**, *25*, 422.
(25) Mativetsky, J. M.; Pace, G.; Elbing, M.; Rampi, M. A.; Mayor, M.; Samorì, P. *J. Am. Chem. Soc.* **2008**, *130*, 9192.
(26) Castellanos, S.; Goulet-Hanssens, A.; Zhao, F.; Dikhtiarenko, A.; Pustovarenko, A.; Hecht, S.; Gascon, J.; Kapteijn, F.; Bléger, D. *Chem. - Eur. J.* **2016**, *22*, 746.
(27) Ferri, V.; Elbing, M.; Pace, G.; Dickey, M. D.; Zharnikov, M.; Samorì, P.; Mayor, M.; Rampi, M. A. *Angew. Chem., Int. Ed.* **2008**, *47*, 3407.
(28) Döbbelin, M.; Ciesielski, A.; Haar, S.; Osella, S.; Bruna, M.; Minoia, A.; Grisanti, L.; Mosciatti, T.; Richard, F.; Prasetyanto, E. A.; De Cola, L.; Palermo, V.; Mazzaro, R.; Morandi, V.; Lazzaroni, R.; Ferrari, A. C.; Beljonne, D.; Samorì, P. *Nat. Commun.* **2016**, *7*, 11090.
(29) Mukhopadhyay, R. D.; Praveen, V. K.; Hazra, A.; Maji, T. K.; Ajayaghosh, A. *Chem. Sci.* **2015**, *6*, 6583.
(30) Babu, S. S.; Praveen, V. K.; Ajayaghosh, A. *Chem. Rev.* **2014**, *114*, 1973.
(31) Velema, W. A.; Szymanski, W.; Feringa, B. L. *J. Am. Chem. Soc.* **2014**, *136*, 2178.
(32) Broichhagen, J.; Frank, J. A.; Trauner, D. *Acc. Chem. Res.* **2015**, *48*, 1947.
(33) Woolley, G. A. *Acc. Chem. Res.* **2005**, *38*, 486.
(34) Schütt, M.; Krupka, S. S.; Milbradt, A. G.; Deindl, S.; Sinner, E.-K.; Oesterhelt, D.; Renner, C.; Moroder, L. *Chem. Biol.* **2003**, *10*, 487.
(35) Stein, M.; Middendorp, S. J.; Carta, V.; Pejo, E.; Raines, D. E.; Forman, S. A.; Sigel, E.; Trauner, D. *Angew. Chem., Int. Ed.* **2012**, *51*, 10500.
(36) Chen, W. P. *Process Biochem.* **1980**, *15*, 36.
(37) Graham Solomons, J. T.; Zimmerly, E. M.; Burns, S.; Krishnamurthy, N.; Swan, M. K.; Krings, S.; Muirhead, H.; Chirgwin, J.; Davies, C. *J. Mol. Biol.* **2004**, *342*, 847.
(38) Terada, T.; Mukae, H.; Ohashi, K.; Hosomi, S.; Mizoguchi, T.; Uehara, K. *Eur. J. Biochem.* **1985**, *148*, 345.
(39) Fischer, G.; Schmid, F. X. *Biochemistry* **1990**, *29*, 2205.
(40) Balbach, J.; Schmid, F. X. In *Mechanisms of protein folding*; Pain, R. H., Ed.; Oxford University Press: Oxford, 2000; pp 212−249.
(41) Herder, M.; Pätzel, M.; Grubert, L.; Hecht, S. *Chem. Commun.* **2011**, *47*, 460.
(42) Goswami, S.; Ghosh, K.; Halder, M. *Tetrahedron Lett.* **1999**, *40*, 1735.
(43) Goodman, A.; Breinlinger, E.; Ober, M.; Rotello, V. M. *J. Am. Chem. Soc.* **2001**, *123*, 6213.
(44) Vollmer, M. S.; Clark, T. D.; Steinem, C.; Ghadiri, M. R. *Angew. Chem., Int. Ed.* **1999**, *38*, 1598.
(45) Lohse, M.; Nowosinski, K.; Traulsen, N. L.; Achazi, A. J.; von Krbek, L. K. S.; Paulus, B.; Schalley, C. A.; Hecht, S. *Chem. Commun.* **2015**, *51*, 9777.
(46) Arroyave, F. A.; Ballester, P. *J. Org. Chem.* **2015**, *80*, 10866.
(47) Hallett-Tapley, G. L.; D'Alfonso, C.; Pacioni, N. L.; McTiernan, C. D.; González-Béjar, M.; Lanzalunga, O.; Alarcon, E. I.; Scaiano, J. C. *Chem. Commun.* **2013**, *49*, 10073.
(48) Titov, E.; Lysyakova, L.; Lomadze, N.; Kabashin, A. V.; Saalfrank, P.; Santer, S. *J. Phys. Chem. C* **2015**, *119*, 17369.
(49) Simoncelli, S.; Aramendía, P. F. *Catal. Sci. Technol.* **2015**, *5*, 2110.
(50) Đorđević, L.; Marangoni, T.; Miletić, T.; Rubio-Magnieto, J.; Mohanraj, J.; Amenitsch, H.; Pasini, D.; Liaros, N.; Couris, S.; Armaroli, N.; Surin, M.; Bonifazi, D. *J. Am. Chem. Soc.* **2015**, *137*, 8150.
(51) Marangoni, T.; Bonifazi, D. *Nanoscale* **2013**, *5*, 8837.
(52) Llanes-Pallas, A.; Yoosaf, K.; Traboulsi, H.; Mohanraj, J.; Seldrum, T.; Dumont, J.; Minoia, A.; Lazzaroni, R.; Armaroli, N.; Bonifazi, D. *J. Am. Chem. Soc.* **2011**, *133*, 15412.
(53) Yoosaf, K.; Llanes-Pallas, A.; Marangoni, T.; Belbakra, A.; Marega, R.; Botek, E.; Champagne, B.; Bonifazi, D.; Armaroli, N. *Chem. - Eur. J.* **2011**, *17*, 3262.
(54) Marangoni, T.; Mezzasalma, S. A.; Llanes-Pallas, A.; Yoosaf, K.; Armaroli, N.; Bonifazi, D. *Langmuir* **2011**, *27*, 1513.
(55) Llanes-Pallas, A.; Palma, C.; Piot, L.; Belbakra, A.; Listorti, A.; Prato, M.; Samori, P.; Armaroli, N.; Bonifazi, D. *J. Am. Chem. Soc.* **2009**, *131*, 509.
(56) Llanes-Pallas, A.; Matena, M.; Jung, T.; Prato, M.; Stöhr, M.; Bonifazi, D. *Angew. Chem., Int. Ed.* **2008**, *47*, 7726.
(57) Feibush, B.; Figueroa, A.; Charles, R.; Onan, K. D.; Feibush, P.; Karger, B. L. *J. Am. Chem. Soc.* **1986**, *108*, 3310.
(58) Hamilton, A. D.; Van Engen, D. *J. Am. Chem. Soc.* **1987**, *109*, 5035.
(59) Vögtle, F.; Gorka, M.; Hesse, R.; Ceroni, P.; Maestri, M.; Balzani, V. *Photochem. Photobiol. Sci.* **2002**, *1*, 45.
(60) Conti, I.; Garavelli, M.; Orlandi, G. *J. Am. Chem. Soc.* **2008**, *130*, 5216.
(61) Takamiya, N.; Tada, M.; Kishimoto, T.; Takano, T.; Sato, Y. *Bull. Sci. Eng. Res.* **1986**, *114*, 12.
(62) Bandara, H. M. D.; Burdette, S. C. *Chem. Soc. Rev.* **2012**, *41*, 1809.
(63) Kuzmic, P. *Anal. Biochem.* **1996**, *237*, 260.
(64) Giannozzi, P.; Baroni, S.; Bonini, N.; Calandra, M.; Car, R.; Cavazzoni, C.; Ceresoli, D.; Chiarotti, G. L.; Cococcioni, M.; Dabo, I.; Dal Corso, A.; de Gironcoli, S.; Fabris, S.; Fratesi, G.; Gebauer, R.; Gerstmann, U.; Gougoussis, C.; Kokalj, A.; Lazzeri, M.; Martin-Samos, L.; Marzari, N.; Mauri, F.; Mazzarello, R.; Paolini, S.; Pasquarello, A.; Paulatto, L.; Sbraccia, C.; Scandolo, S.; Sclauzero, G.; Seitsonen, A. P.;

Smogunov, A.; Umari, P.; Wentzcovitch, R. M. *J. Phys.: Condens. Matter* **2009**, *21*, 395502.

(65) Perdew, J. P.; Burke, K.; Ernzerhof, M. *Phys. Rev. Lett.* **1996**, *77*, 3865.

(66) Turanský, R.; Konôpka, M.; Doltsinis, N. L.; Štich, I.; Marx, D. *Phys. Chem. Chem. Phys.* **2010**, *12*, 13922.

(67) Dubecký, M.; Derian, R.; Mitas, L.; Štich, I. *J. Chem. Phys.* **2010**, *133*, 244301.

(68) Jonsson, H.; Mills, K. W. J. *Classical and Quantum Dynamics in Condensed Phase Simulations*; Berne, B. J., Ciccotti, G., Coker, D. F., Eds.; World Scientific: Singapore, 1998.

(69) Henkelman, G.; Uberuaga, B. P.; Jónsson, H. J. *J. Chem. Phys.* **2000**, *113*, 9901.

(70) Henkelman, G.; Jónsson, H. *J. Chem. Phys.* **2000**, *113*, 9978.

(71) Neukirch, A. J.; Shamberger, L. C.; Abad, E.; Haycock, B. J.; Wang, H.; Ortega, J.; Prezhdo, O. V.; Lewis, J. P. *J. Chem. Theory Comput.* **2014**, *10*, 14.

(72) Wang, R.; Jin, C.; Zhu, X.; Zhou, L.; Xuan, W.; Liu, Y.; Liu, Q.; Tan, W. *J. Am. Chem. Soc.* **2017**, *139*, 9104.

(73) Stafforst, T.; Hilvert, D. *Angew. Chem., Int. Ed.* **2010**, *49*, 9998.

(74) Goldau, T.; Murayama, K.; Brieke, C.; Steinwand, S.; Mondal, P.; Biswas, M.; Burghardt, I.; Wachtveitl, J.; Asanuma, H.; Heckel, A. *Chem. - Eur. J.* **2015**, *21*, 2845.

(75) Matsunaga, D.; Asanuma, H.; Komiyama, M. *J. Am. Chem. Soc.* **2004**, *126*, 11452.

(76) Freeman, N. S.; Moore, C. E.; Wilhelmsson, L. M.; Tor, Y. *J. Org. Chem.* **2016**, *81*, 4530.